

## A BISYMMETRIC SPIRAL MAGNETIC FIELD AND THE SPIRAL ARMS IN OUR GALAXY

Y. SOFUE

Nobeyama Radio Observatory, Tokyo Astronomical Observatory, University of Tokyo

AND

M. FUJIMOTO

Department of Physics and Astrophysics, Nagoya University

Received 1981 December 21; accepted 1982 August 2

### ABSTRACT

An analysis is made of Faraday rotation measures (RMs) of extragalactic radio sources. It is shown that a large-scale magnetic field in our Galaxy is oriented along the spiral arms. The field lines change their direction from one arm to the next across the neutral line in the interarm region. The loci of maximum field strength trace the spiral arms defined by H II regions. Characteristic features of the RM distribution on the sky are well reproduced by a model in which the magnetic field is in a bisymmetric, two-armed logarithmic spiral configuration satisfying the flux conservation along the arm: the magnetic lines of force flow into the one half of the Galaxy in a spiral way and flow out from the diametrically opposite half.

*Subject headings:* galaxies: Milky Way — galaxies: structure — interstellar: magnetic fields — radio sources: general

### I. INTRODUCTION

A bisymmetric open-spiral configuration of large-scale magnetic fields in nearby spiral galaxies has been found through several analyses of Faraday rotation of the linearly polarized radio emission (Tosa and Fujimoto 1978; Sofue, Takano, and Fujimoto 1980; Sofue and Takano 1981; Beck 1982; Klein *et al.* 1982; see also Table 1). The knowledge of field configurations in galaxies should provide a promising clue to the origin of the galactic magnetic fields and their implications for the evolution and dynamics of galaxies.

The magnetic field in our Galaxy, especially in the solar neighborhood, has been extensively studied by analyzing the rotation measures (RMs) of the Faraday effect on pulsars and extragalactic radio sources (see Verschuur 1979 and the wealth of literature cited therein). The works by Simard-Normandin and Kronberg (1979, 1980) and by Inoue and Tabara (1981) are based on the largest amount of RM data available at that time. The former authors propose a bisymmetric spiral field which reverses its direction from one arm to the next (see also Thomson and Nelson 1980), while Inoue and Tabara are in doubt about the bisymmetric nature, claiming, rather, a circular field along the solar circle without any field reversal within it.

In this paper we analyze the RM data of extragalactic radio sources compiled by Tabara and Inoue (1980) to determine whether or not the bisymmetric field concept can apply to our Galaxy. We examine a current theory of bisymmetric spiral magnetic field in the disk of a

galaxy proposed by Fujimoto and Tosa (1980) by taking into account our results from the RM analysis.

### II. DISTRIBUTION OF ROTATION MEASURES

Tabara and Inoue (1980) have compiled radio polarization data for 1510 radio sources and have determined their RMs. We will make use of these RM data in the following analysis, in which, however, we exclude the sources with absolute RMs greater than  $300 \text{ rad m}^{-2}$  or with mean errors greater than  $10 \text{ rad m}^{-2}$  that have been produced in the determination of RM. We also exclude some sources that are identified with galactic objects like supernova remnants.

Inoue and Tabara (1981) have studied the magnetic field in the solar vicinity by using their own data, but they excluded those sources with  $|\text{RM}| \geq 100 \text{ rad m}^{-2}$ . However, since we are interested in a larger-scale field configuration of the Galaxy, we cannot ignore the contribution from the distant spiral arms. In fact, many of the radio sources at low latitudes ( $|b| < 20^\circ$ ) have  $|\text{RM}| \approx 100 \text{ rad m}^{-2}$ . For example,  $|\text{RM}| \approx 300 \text{ rad m}^{-2}$  is realized when the radio wave propagates over 5 kpc along a magnetic line of force of 3 microgauss and electron density of  $0.03 \text{ cm}^{-3}$  (e.g., Manchester and Taylor 1977). For this reason we include in our analysis the radio sources of  $|\text{RM}| > 100 \text{ rad m}^{-2}$  which Inoue and Tabara (1981) discarded.

Figure 1 shows the distribution of the radio sources thus selected and used in the present analysis. To search

## BISYMMETRIC SPIRAL MAGNETIC FIELD

723

TABLE 1  
LARGE-SCALE MAGNETIC FIELD CONFIGURATIONS IN OUR GALAXY AND NEARBY GALAXIES

Galaxy	Morphological Type	Field Configuration	Field Strength ( $\mu\text{G}$ )	Pitch Angle	Method	References
Our Galaxy .....	Sb	bisymmetric spiral	3 <sup>a</sup>	$-14^\circ$ $\sim -5^\circ$	RM of pulsars and extragalactic radio sources	1, 2, and present work
M33 .....	Sc	bisymmetric, open spiral	...	$-20^\circ$	RM of linearly polarized emission of the galaxy	3
M51 .....	Sc	bisymmetric, open spiral	5	$20^\circ$	RM of linearly polarized emission of the galaxy	3, 4
M81 .....	Sb	bisymmetric, open spiral	3	$23^\circ$	RM of linearly polarized emission of the galaxy	3
MGC 6946 .....	Sc	bisymmetric, open spiral	15	$-30^\circ$	RM of linearly polarized emission of the galaxy	5
M31 .....	Sb	circular along the "10 kpc ring," possibly bisymmetric at $R \geq 13$ kpc	2.2	$0^\circ$	RM of linearly polarized emission of the galaxy	6, 7

<sup>a</sup>In the solar vicinity.

REFERENCES.—(1) Thomson and Nelson 1980. (2) Simard-Normandin and Kronberg 1979, 1980. (3) Sofue, Takano, and Fujimoto 1980. (4) Tosa and Fujimoto 1978. (5) Klein *et al.* 1981. (6) Sofue and Takano 1981. (7) Beck 1981.

for a large-scale structure in the RM distribution in Figure 1 and to reduce the effect of small-scale irregularities, we obtain a smoothed RM distribution. Here

*smoothed* RM implies a Gaussian-weighted mean of RM for sources around a position we consider. The resulting distribution map looks like the sky observed with a

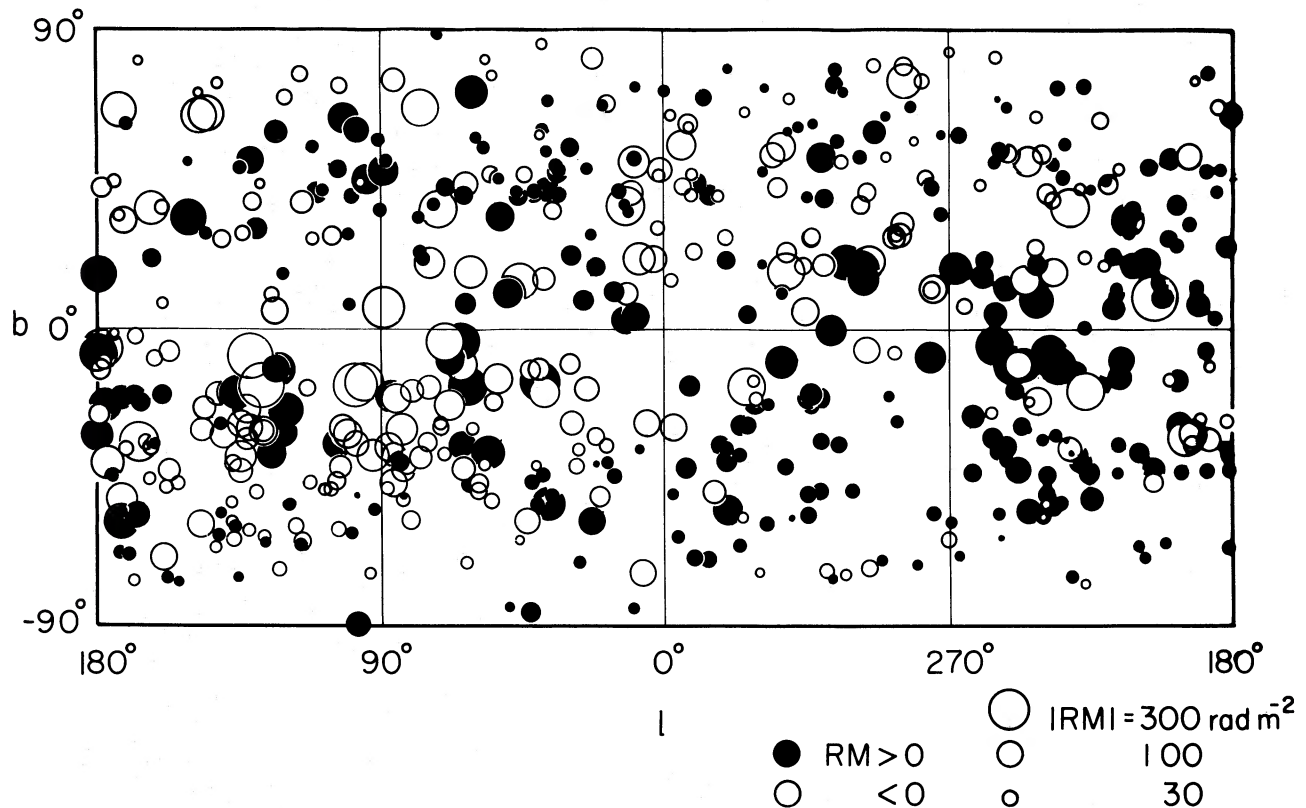


FIG. 1.—Distribution of rotation measures (RM) of radio sources in the galactic coordinate system. Galactic objects like supernova remnants and sources with  $|\text{RM}|$  greater than  $300 \text{ rad m}^{-2}$  are excluded. Positive RMs are indicated with filled circles, and negative ones with open circles.

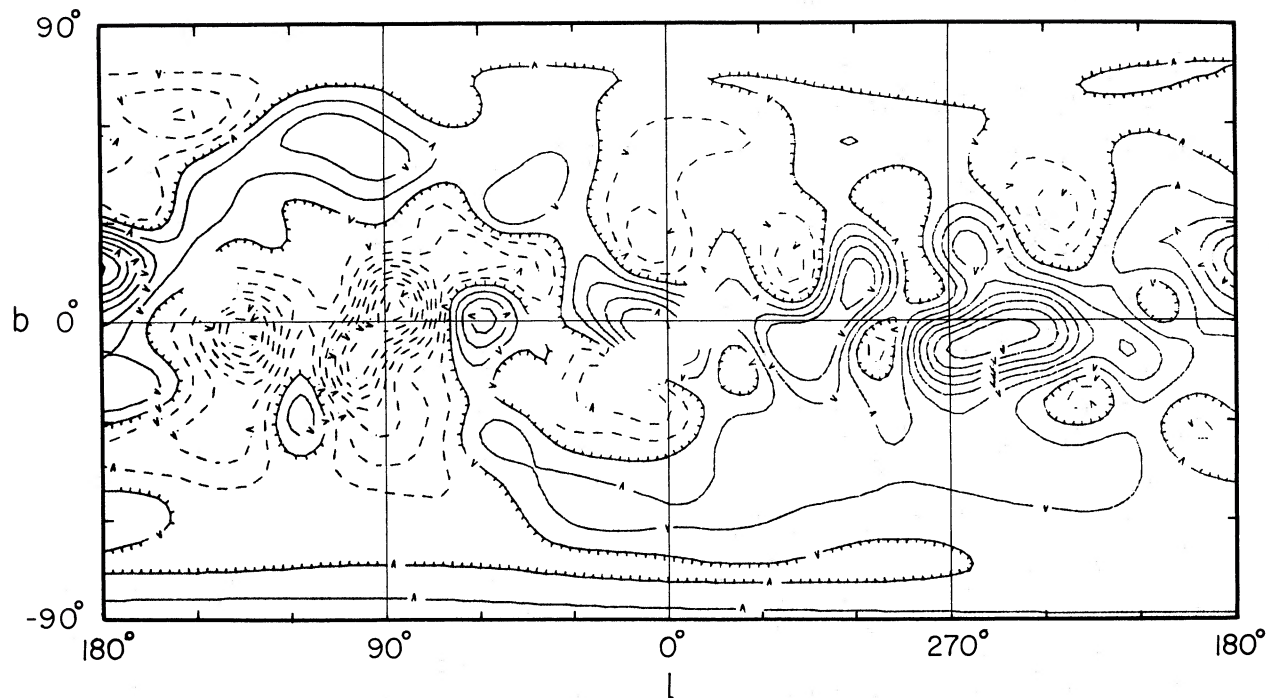


FIG. 2a

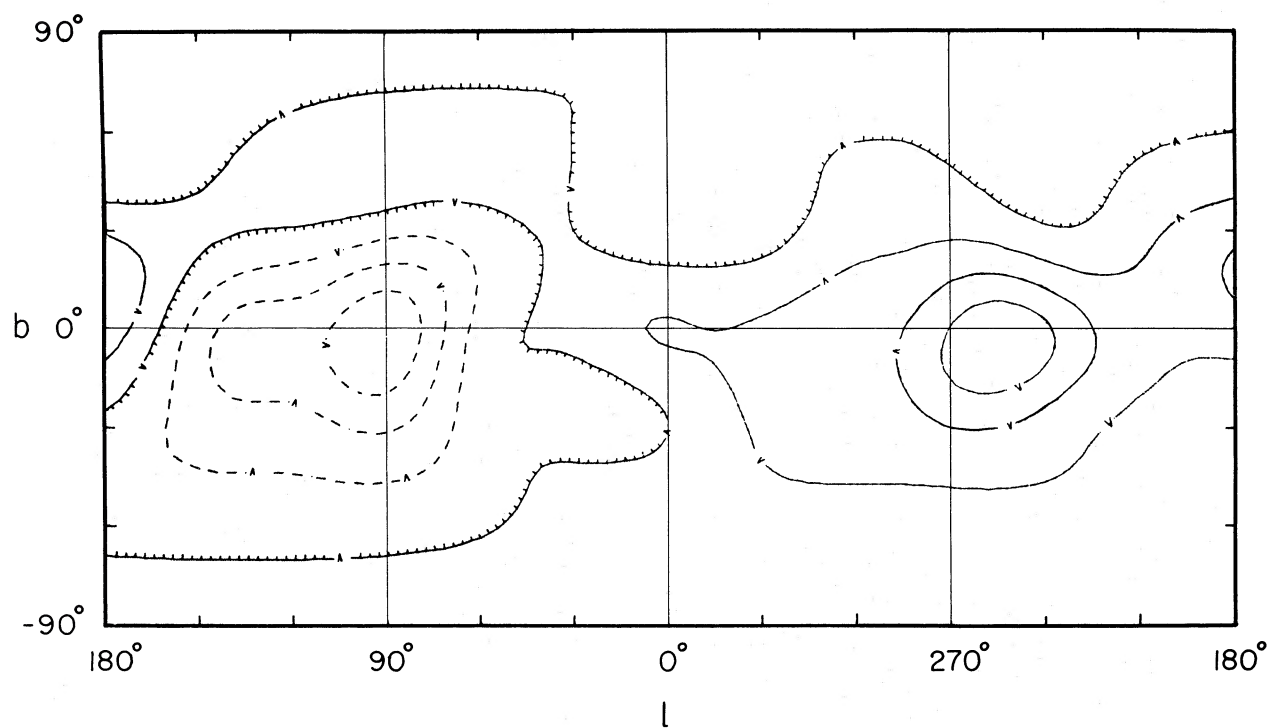


FIG. 2b

FIG. 2.—(a) Smoothed distribution of the observed RMs in Fig. 1 by a Gaussian beam of full half-width of  $\Theta = 20^\circ$ . The contour intervals are  $20 \text{ rad m}^{-2}$  each. Positive RMs are indicated by solid-line contours, and negative ones with dashed-line contours. The contours at  $\text{RM} = 0$  are indicated with tick marks pointing toward negative RM regions, and the arrows on the contours point toward less RM sides. Several regions with no contours are those in which no source is found within our beamwidth. (b) Same as Fig. 2a but smoothed to a full beamwidth of  $40^\circ$ .

Gaussian beam. Figure 2a shows a distribution of RMs smoothed to a full half-width of  $\Theta = 20^\circ$ . Figure 2b shows the same map but smoothed to a beamwidth of  $\theta = 40^\circ$ .

Characteristic features observed in Figures 2a and 2b are summarized as follows:

1. A wide negative region of RM is centered at  $l \approx 90^\circ$  and  $b \approx 0^\circ$ , and a wide positive region at  $l \approx 260^\circ$  and  $b \approx 0^\circ$  (Fig. 2b). This feature is due to a local magnetic field in the solar vicinity which runs from  $l \approx 260^\circ, b = 0^\circ$  toward  $l \approx 90^\circ, b = 0^\circ$ , as has been reported repeatedly by many authors (see, e.g., Verschuur 1979). In Figure 2b smaller-scale structures as seen in Figure 2a are smeared out.

2. Maxima and minima of RM are found in smaller scale at low latitudes ( $|b| < 20^\circ$ ) in the directions of the inner arms (Fig. 2a): A maximum at  $l = 56^\circ$  is found in the tangential direction to the Sagittarius arm; a mini-

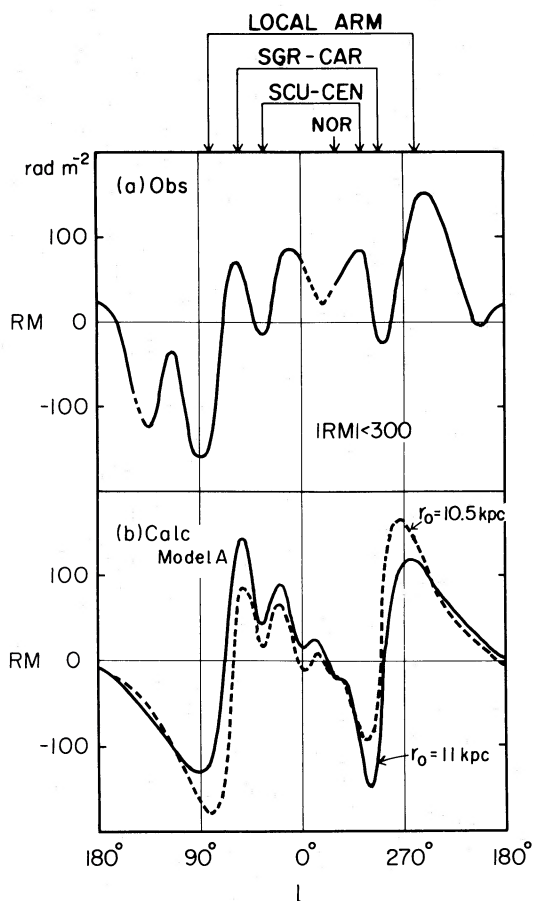


FIG. 3.—(a) A crosscut of the observed RM distribution in Fig. 2a along the galactic plane. Maxima and minima of RMs, corresponding to the spiral arms, are indicated with the arrows on the top. The mean error of the curved line is approximately  $\pm 30 \text{ rad m}^{-2}$ . (b) A crosscut of the RM distribution in Fig. 2a along the galactic plane, calculated on the basis of a bisymmetric open-spiral configuration of magnetic field.

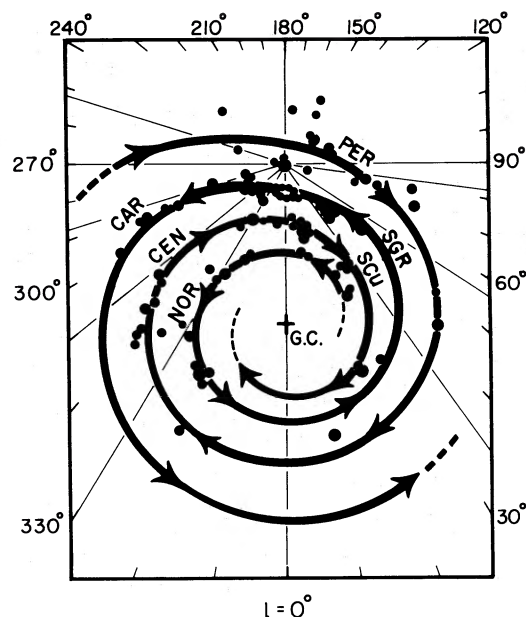


FIG. 4.—Possible, two-armed, bisymmetric spirals (thick lines) fitted to the distribution of H II regions (filled circles) given by Geogelin and Geogelin (1976). The arrows indicate the direction of magnetic field as inferred from Figs. 2 and 3.

imum at  $l = 35^\circ$ , to the Carina arm; a minimum at  $l = 310^\circ$ , to the Centaurus arm; and a minimum at  $l = 330^\circ$ , possibly corresponding to the Norma arm. To see the situation more clearly we show in Figure 3a a crosscut of Figure 2a along the galactic plane, where we indicate the tangential directions to the inner arms by arrows. The statistical error of the smoothed line is about  $\pm 30 \text{ rad m}^{-2}$  on the average. The wavy nature of Figure 3 can, therefore, be regarded as real. The local maximum and minimum arise alternately over the galactic longitude, and their positions are exactly in the tangential directions of the inner arms. These characteristics of the smoothed distribution of RMs can be qualitatively understood in terms of the large-scale galactic magnetic field which is oriented along the arm and reverses its direction when we go from one arm to the next. The reversals of the field direction occur between the Local arm and the Sagittarius-Carina arm, between the Sagittarius-Carina arm and the Scutum-Centaurus arm, and possibly between the Norma and Centaurus arms. Such a field configuration is consistent with that proposed by Simard-Normandin and Kronberg (1980).

Figure 4 shows two bisymmetric spirals which can possibly trace the distribution of H II regions given by Geogelin and Geogelin (1976). The arrows indicate the directions of the magnetic field in the arms inferred from our data. The Sun is located at an inner edge of the Perseus arm where the field line is directed from  $l = 260^\circ$ ,

$b = 0^\circ$  toward  $l = 85^\circ$ ,  $b = 0^\circ$ . The nearest neutral line of the field lies between the Sun and the Sagittarius arm.

3. At high latitudes ( $|b| \geq 30^\circ$ ), particularly in the northern hemisphere, the RM distribution is rather complicated and cannot be understood simply by a regular magnetic field along the spiral arms. A local irregular field may be related to it. Magnetic fields outside the galactic disk, as in the galactic halo and intergalactic space (Sofue, Fujimoto, and Kawabata 1979), may also play some role in RMs at high latitudes.

The above results may be affected by the upper limit of  $|RM|$  chosen for the sources in the analysis. We note that the argument for the uniform circular field by Inoue and Tabara (1981) has been made on the basis of RMs whose absolute values are less than  $100 \text{ rad m}^{-2}$ . Their data analysis might miss the RM contribution from the inner arms at low latitudes. Nevertheless, it is true, as Inoue and Tabara (1981) claim, that the larger the  $|RM|$  values, the greater are their uncertainties. Indeed the distribution of RMs for the sources of  $300 < |RM| < 1000 \text{ rad m}^{-2}$  is almost random on the sky. These are the reasons why we have taken into account the sources with  $|RM| \leq 300 \text{ rad m}^{-2}$  and ignored those with  $|RM| > 300 \text{ rad m}^{-2}$ .

### III. THE BISYMMETRIC SPIRAL MODEL OF THE GALACTIC MAGNETIC FIELD

To see more clearly whether or not the bisymmetric field configuration in Figure 4 is reasonable, we calculate the distribution of RMs projected onto the sky as expected from a model of Fujimoto and Tosa (1980).

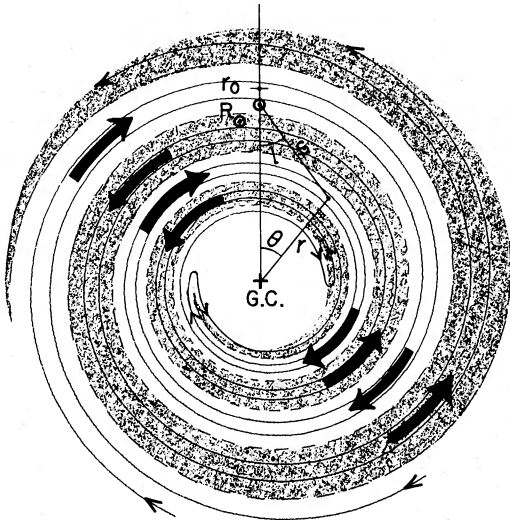


FIG. 5.—Bisymmetric open-spiral magnetic fields used for our model computations of RM in Fig. 6. The field directions are indicated with the arrows. The geometrical meanings of  $r_0$ ,  $p = \tan^{-1} 1/\beta$ , and  $R_\odot$  can be read from this figure.

The radial and azimuthal components of a magnetic field in a bisymmetric logarithmic spiral configuration are given conveniently through

$$B_r = -\frac{f(r)}{r} \cos\left(\theta + \beta \ln \frac{r}{r_0}\right) \quad (1)$$

and

$$B_\theta = \frac{f(r)\beta}{r} \cos\left(\theta + \beta \ln \frac{r}{r_0}\right), \quad (2)$$

with  $\beta \gg 1$ . Here  $r$  and  $\theta$  are, respectively, the galactocentric distance and azimuthal angle around the galactic center;  $\beta$  is a constant given by  $\beta = 1/\tan p$  with  $p$  the pitch angle of the spiral. The symbol  $r_0$  is a constant, and  $f(r)$  is a smooth function of  $r$  (Fig. 5).

The rotation measure (in  $\text{rad m}^{-2}$ ) on the sky in a direction  $(l, b)$  is given by

$$\begin{aligned} \text{RM}(l, b) = & -810 \int_0^\infty N_e(r) X(r) \exp\left(-\frac{z^2}{D_e^2}\right) \\ & \times \exp\left(-\frac{z^2}{D_B^2}\right) (\cos b) \cos\left(\theta + \beta \ln \frac{r}{r_0}\right) \\ & \times \left[ \sin(\theta + l) + \frac{1}{\beta} \cos(\theta - l) \right] ds, \quad (3) \end{aligned}$$

where

$$X(r) = f(r)/r, \quad z = s(\tan b),$$

$$r = (s^2 + R_\odot^2 - 2sR_\odot \cos l)^{1/2}, \quad \sin \theta = s/r(\sin l),$$

and

$$\cos \theta = (R_\odot^2 + r^2 - s^2)/(2rR_\odot).$$

Here  $s$  (in kpc) is a distance from the Sun projected onto the galactic plane;  $z$  is the height from the galactic plane;  $R_\odot$  is the distance of the Sun from the center, taken as 10 kpc (Fig. 5). The quantities  $N_e(r)$  (in  $\text{cm}^{-3}$ ) and  $X(r)$  (in microgauss) denote the electron density and field amplitude in the galactic plane, respectively.

The distributions of the electron density and field strength in the  $z$ -direction are assumed to be Gaussian, with their scale thickness  $D_e$  and  $D_B$ , respectively. In the following we take  $D_e = D_B = 0.5\text{--}1.0$  kpc, according to the estimate of the thickness of the electron disk (Manchester and Taylor 1977) and the magnetic disk (Sofue 1976; Inoue and Tabara 1981). The spiral parameter  $\beta$  is taken to be  $-12$ , which yields a pitch angle of  $-5^\circ$ , and the maximum position of field strength in the

solar vicinity is taken to be at  $r_0 = 11$  kpc. Figure 5 illustrates some of the spiral field used in our model. The parameters  $\beta$  and  $r_0$  of spirals have been adopted so that the arms defined by H II regions (Fig. 4) are well fitted by two-armed logarithmic spirals. (Note that Georgelin and Georgelin 1976 have fitted the H II regions by four-armed spirals of pitch angle  $-14^\circ$ .)

As to the radial variation of electron density and mean field strength we consider the following two simple cases:

$$\text{Model A} \begin{cases} N_e(r) = 0.03 R_\odot/r \text{ cm}^{-3} \\ X(r) = 3 R_\odot/r \text{ microgauss} \end{cases} \quad \text{at } 4 \leq r \leq 15 \text{ kpc} \quad (4)$$

and

$$\text{Model B} \begin{cases} N_e(r) = 0.03 \text{ cm}^{-3} \\ X(r) = 3 \text{ microgauss} \end{cases} \quad \text{at } 4 \leq r \leq 15 \text{ kpc}. \quad (5)$$

In both cases we assume that  $N_e(r) = X(r) = 0$  at  $r < 4$  kpc and at  $r > 15$  kpc. The local values,  $N_e(R_\odot) = 0.03 \text{ cm}^{-3}$  and  $X(R_\odot) = 3 \text{ microgauss}$ , are taken from Manchester and Taylor (1977). When  $X(r) \propto 1/r$  or  $f(r) = \text{const}$  (model A), the magnetic field increases toward the galactic center along the arm, and when  $X(r) = \text{const}$  or  $f(r) \propto r$  (model B), it remains constant.

Now we integrate equation (3) at every  $5^\circ$  in the  $(l, b)$ -coordinates, and we smooth them with a Gaussian beam of a full half-width of  $\Theta = 20^\circ$ . The resulting distributions of RM( $l, b$ ) for models A and B with  $D_e = D_B = 0.5$  kpc are shown in Figures 6a and 6b in the form of contour maps. We find that model A (Fig. 6a) can reproduce many of the global characteristics observed from  $l = 250^\circ$  through  $150^\circ$  at low latitudes in Figure 2a. The positive and negative regions of RM appear alternately with galactic longitudes, resembling those in Figure 2a. However, a local positive minimum is found at  $l = 35^\circ, b = 0^\circ$  in the tangential direction to the Scutum arm where RM must be negative because the field is directed away from us (see Figs. 4 and 5). This result is due to our smoothing of the computed data over the finite beamwidth, which is a little too large compared with the apparent cross section of the Scutum arm at 5–9 kpc from the Sun in the direction  $l = 35^\circ, b = 0^\circ$ : the rotation measures around the arm and its back- and foreground ones are involved in a single beam.

The crosscut of Figure 6a along the galactic plane (Fig. 3b) is more heuristic when compared with Figure 3a. The positions and phases of the computed maxima and minima are in good coincidence with those observed along galactic longitudes in Figure 3a, although some amplitudes remain open to discussion.

We notice that the local extrema of RM in Figure 3a appear antisymmetrically (if the one at  $l \approx 100^\circ$  is excluded) with respect not to  $l = 0^\circ$  but to  $l = -10^\circ$ . From this fact and the above discussion, we can understand that the magnetic field lines are distributed not in circles but in two spirals with a pitch angle of  $\sim 10^\circ$ . The magnetic field reverses its direction when we go from an arm to the neighboring ones (Figs. 4 and 5).

The bump of RM at  $l = 100^\circ$  in Figure 3a is due to the mixture of sources of positive rotation measures at  $l \approx 100^\circ, b \approx -20^\circ$  (filled circles in Fig. 1). It may result from a local fluctuation of the interstellar magnetic field: the field lines in the Perseus arm branch off from its southern part ( $b < 0$ ) and are directed toward us. In fact, the polarization degree of optical starlight (Mathewson and Ford 1970) seems to be small at  $l \approx 110^\circ, b = -20^\circ$ , suggesting that the field lines are directed mostly toward us. Even if the galactic magnetic field is circular, the bump is anomalous, superposed on the smooth distribution of RMs. We exclude this RM anomaly from our discussions and keep in mind that our model fitting and later conclusion are made neglecting the local field fluctuation in the direction of  $l = 100^\circ, b = -20^\circ$ .

Model B (Fig. 6b) seems to reproduce the observed features more poorly; this is particularly evident from  $l = 300^\circ$  through  $l = 60^\circ$ . When we make a crosscut of Figure 6b along the galactic plane and it is compared with Figure 2a, our choice of model A, rather than B, will be recognized. We may therefore conclude that model A, with increasing electron density and increasing magnetic field toward the inner region, is more plausible than model B, with constant  $N_e(r)$  and  $X(r)$ . We note that in model A the magnetic flux in a spiral arm is conserved along the arm in the limit of  $1/|\beta| \ll 1$ .

We have examined also a case in which  $N_e$  and  $X$  are more steeply varying functions of  $r$  as it is proportional to  $1/r^2$ . However, the result gives too large  $|\text{RM}|$ -values toward the inner arms, and it cannot be accepted. We have further examined other cases with different spiral parameters and disk thickness. A comparison with the observations gives that  $D_e$  and  $D_B$  lie around 0.5 kpc. A set of parameters  $p (= \tan^{-1} 1/\beta) = -5^\circ$  and  $r_0 = 11$  kpc in equations (1) and (2) gives an overall good result, insofar as we assume the bisymmetric spiral field. We did not examine a case with four-armed spirals, as proposed by Georgelin and Georgelin (1976), for it involves too many parameters in describing the field distribution.

#### IV. DISCUSSION

A bisymmetric spiral configuration is derived as the most reliable model for the global magnetic field in our Galaxy. The present result supports the model by Thomson and Nelson (1980) and Simard-Normandin and Kronberg (1980), regarding their field configuration

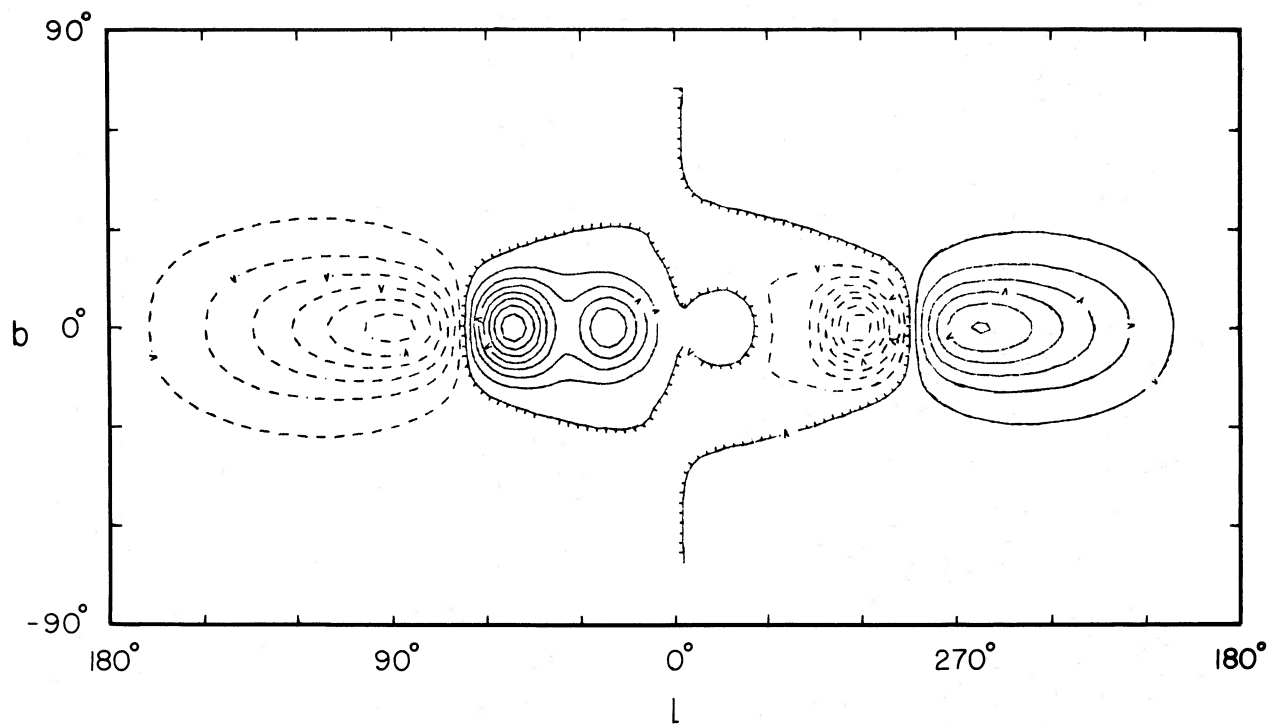


FIG. 6a

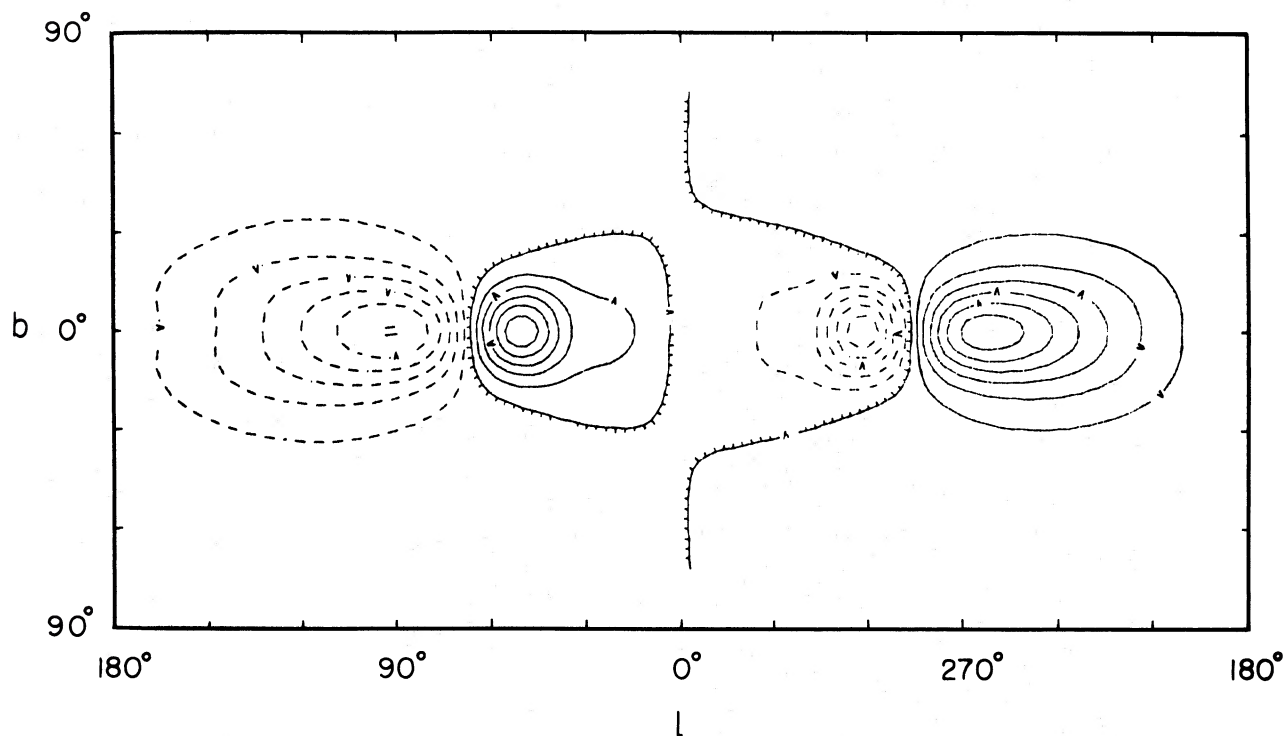


FIG. 6b

FIG. 6.—(a) Calculated RM distribution smoothed to a full beamwidth of  $\theta = 20^\circ$ , using the spirals in Fig. 5 for model A in the text. (b) Same as Fig. 6a but for model B.

as representing a solar local portion of our Figures 4 and 5.

The bisymmetric nature with field reversals in between spiral arms seems to apply for most of the inner arms, namely, for the Local arm, Sagittarius-Carina arm, Scutum-Centaurus arm, and Norma arm. A simulation of the RM distribution on the sky based on a model of the bisymmetric open-spiral field by Fujimoto and Tosa (1980) can reproduce well many of the observed characteristics at  $|b| \leq 30^\circ$ . It is rather striking that such a very simple model can explain many of the observed features.

We remember that the choice of our spiral field model is made neglecting the RM bump at  $l=100^\circ$  in Figure 2a. In view of the results of Thomson and Nelson (1980) and Simard-Normandin and Kronberg (1979) and those in Table 1, we incline toward the view that the present model is not so unrealistic and that it provides more help in studying the magnetic field problem of our Galaxy. The RM anomaly at  $l=100^\circ$  seems to be a large-scale fluctuation of the galactic field.

According to the hydromagnetic theory on the spiral condensation of interstellar gas (Fujimoto and Tosa 1980), the positional relationship between the maximum gas condensation and maximum field strength depends sensitively on the angular velocity  $\Omega$  of the field pattern. The present result, that the maximum field strength occurs at the loci of the maximum gas density, gives  $\Omega \approx 0$  and/or the slow angular velocity of the field pattern.

The bisymmetric spiral field in the Galaxy and those found in nearby spiral galaxies (Table 1) are consistent with the hypothesis of a primordial origin of the galactic magnetic fields which would predict that the magnetic lines of force have been wound up from intergalactic space into the galaxy disk (Ôki, Fujimoto, and Hitotuyanagi 1964; Zel'dovich 1964; Piddington 1964, 1972). It is interesting to note that the primordial origin is consistent with our result of  $\Omega \approx 0$ , since the galactic field line must connect smoothly with the intergalactic

field line with no rotation  $\Omega = 0$  or, if it exists, with very slow rotation  $\Omega \approx 0$  compared with the galactic disk. In our best case, model A, the field strength varies as  $1/r$ , and the disk thickness is constant, which ensures the flux conservation along the spiral arm at  $r \geq 4$  kpc.

The galactic dynamo action proposed so far (Parker 1971, 1979) seems to play a minor role in producing such a large-scale spiral magnetic field. A new step toward understanding the origin of magnetic fields may be thus put forward based on the evidence for spiral fields. Some progress in theoretical study of the bisymmetric spiral fields and their implication for the dynamics of disk galaxies has been reported (Fujimoto and Tosa 1980; Sawa and Fujimoto 1980; Fujimoto and Sawa 1981).

The complicated RM distribution observed at high latitudes, especially at  $b > 30^\circ$ , is hard to understand in terms of the present model. We may need a more sophisticated approach taking into account the contribution from local irregular fields, helical components spiraling around the arms, magnetic fields in the galactic halo and those in intergalactic space. A large amplitude warping of the galactic disk in the outer region at  $r \geq 15$  kpc (Verschuur 1973; Davies 1972) could also affect the RM at  $l=90^\circ-130^\circ$  and  $b=20^\circ-40^\circ$ . Since we are interested in a regular field orientation at low latitudes, we relegate a detailed discussion of these effects to another paper. However, readers may refer to a review paper by Verschuur (1979) and to the literature cited therein.

The authors are indebted to Drs. M. Inoue and H. Tabara for their discussions and for making their data available in the form of a magnetic tape. This research has been in part supported by the Scientific Research Fund of the Ministry of Education, Sciences, and Culture under grants 542003 (Y. Sofue, FY 1980, 1981) and 5642004 (M. Fujimoto, FY 1981). Numerical computations were made on a FACOM-M200 at the Institute of Plasma Physics.

#### REFERENCES

- Beck, R. 1982, *Astr. Ap.*, **106**, 121.  
 Davies, R. D. 1972, *M. N. R. A. S.*, **160**, 381.  
 Fujimoto, M., and Sawa, T. 1981, *Pub. Astr. Soc. Japan*, **33**, 265.  
 Fujimoto, M., and Tosa, M. 1980, *Pub. Astr. Soc. Japan*, **32**, 567.  
 Georgelin, Y. M., and Georgelin, Y. P. 1976, *Astr. Ap.*, **49**, 57.  
 Inoue, M., and Tabara, H. 1981, *Pub. Astr. Soc. Japan*, **33**, 603.  
 Klein, U., Beck, R., Buczylowski, U. R., and Wielebinski, R. 1982, *Astr. Ap.*, **108**, 176.  
 Manchester, R. N., and Taylor, J. H. 1977, *Pulsars* (San Francisco: Freeman), p. 133.  
 Mathewson, D. S., and Ford, V. L. 1970, *Mem. R. A. S.*, **74**, 139.  
 Ôki, T., Fujimoto, M., and Hitotuyanagi, Z. 1964, *Progr. Theor. Phys. Suppl.*, No. 31, p. 77.  
 Parker, E. N. 1971, *Ap. J.*, **163**, 255.  
 ———. 1979, *Cosmical Magnetic Fields* (Oxford: Clarendon), chap. 22.  
 Piddington, J. H. 1964, *M. N. R. A. S.*, **128**, 345.  
 Piddington, J. H. 1972, *Cosmic Electrodyn.*, **3**, 129.  
 Sawa, T., and Fujimoto, M. 1980, *Pub. Astr. Soc. Japan*, **32**, 551.  
 Simard-Normandin, M., and Kronberg, P. P. 1979, *Nature*, **279**, 115.  
 ———. 1980, *Ap. J.*, **242**, 74.  
 Sofue, Y. 1976, *Astr. Ap.*, **48**, 1.  
 Sofue, Y., Fujimoto, M., and Kawabata, K. 1979, *Pub. Astr. Soc. Japan*, **31**, 125.  
 Sofue, Y., and Takano, T. 1981, *Pub. Astr. Soc. Japan*, **33**, 47.  
 Sofue, Y., Takano, T., and Fujimoto, M. 1980, *Astr. Ap.*, **91**, 335.  
 Tabara, H., and Inoue, M. 1980, *Astr. Ap. Suppl.*, **39**, 379.  
 Thomson, R. C., and Nelson, A. H. 1980, *M. N. R. A. S.*, **191**, 863.  
 Tosa, M., and Fujimoto, M. 1978, *Pub. Astr. Soc. Japan*, **30**, 315.  
 Verschuur, G. L. 1973, *Astr. Ap.*, **22**, 139.  
 ———. 1979, *Fund. Cosmic Phys.*, **5**, 113.  
 Zel'dovich, Ya. B. 1964, *Soviet Phys.—JETP*, **21**, 656.

M. FUJIMOTO: Department of Physics and Astrophysics, Nagoya University, Nagoya 464, Japan

Y. SOFUE: Nobeyama Radio Observatory, Tokyo Astronomical Observatories, University of Tokyo, Mitaka 181, Tokyo, Japan